ROYAL SOCIETY
OF CHEMISTRY

PAPER

Check for updates

Excited state dipole moments from ΔSCF: a benchmark†

Lukas Paetow and Johannes Neugebauer [ID] *

The molecular electric dipole moment of a given electronic state is a simple indicator for the associated charge distribution, and allows a first assessment of how the molecule is influenced by an oriented external electric field (OEF). If the dipole moments of two energetically close electronic states are significantly different, OEFs can be used to tune the molecular photophysics and photochemistry by modifying the shapes and order of the excited-state potential-energy surfaces. Here, we present a comprehensive benchmark of excited-state dipole moments obtained from ΔSCF methods, which have recently gained renewed attention and offer access to excited-state properties essentially with ground-state technology. We investigate the accuracy of these dipole moments in comparison with TDDFT and wavefunction-based calculations, as well as with literature data. We find that, on average, ΔSCF data do not necessarily improve on TDDFT results, but offer increased accuracy in certain pathological cases. In particular, excited-state dipole moments can be obtained with reasonable accuracy for certain doubly excited states, while these states are not accessible at all for conventional TDDFT calculations. Excited-state dipole moments for charge-transfer states, however, suffer from the DFT overdelocalization error, which can affect a ΔSCF calculation on a charge-separated state more severely than the corresponding TDDFT calculation, since the latter typically starts from a charge-neutral ground-state reference. For push–pull systems like donor–acceptor-substituted polyenes, however, this overdelocalization can lead to beneficial error cancellation with the overestimated charge-transfer observed in the ground state.

1 Introduction

For charge-neutral molecules, the electric dipole is the first non-vanishing term in the multipole expansion of the molecule's charge distribution in a given electronic state. Hence, the knowledge of excited-state dipole moments allows to assess the charge redistribution upon excitation and the charge-transfer character of a given excited state if the corresponding ground-state dipole moment is known as well.[1] This can be the first step towards more detailed analyses like "electrostatic profiling" based on the molecular electrostatic potential[2] or considerations of higher-order multipole moments (or related quantities, see ref. 3). In addition, knowing the dipole moments of various close-lying excited electronic states is highly important in the context of using oriented electric fields as "reagents" in chemistry,[4] as it offers insight into possible tuning mechanisms of photophysical and photochemical pathways by such fields (see, *e.g.*, ref. 5). Such tuning mechanisms

are highly relevant, *e.g.*, in fluorescent indicators that change their emission properties depending on membrane potentials,[6] Stark-effect based flipping of bright and dark states of optical switches in biased metallic nanojunctions,[7] energy-transfer in photosynthetic light-harvesting complexes,[8] or for modulating photochemical isomerization pathways.[9,10]

Ground-state equilibrium dipole moments from density-functional theory (DFT) have been extensively benchmarked by Hait and Head–Gordon,[11] who compared results from various classes of density-functional approximations (DFAs) to those from wavefunction theory. For the latter (as well as for the MP2 component of double hybrids), dipole moments were obtained from finite-field calculations. It was found that the best-performing DFAs (from the class of double hybrid functionals) yield regularized root mean square errors (RMSEs) of about 4%, which is comparable to CCSD, followed by hybrid functionals, many of which give regularized RMSEs of less than 6%. The best (semi-)local functionals still achieve regularized RMSEs of about 8%. The regularization was applied in that study in order to avoid biases due to large relative errors in species with small absolute dipole moments.

For excited-state dipole moments, two popular routes within the framework of DFT exist: time-dependent density functional theory (TDDFT) and ΔSCF. While the former requires the

Theoretische Organische Chemie, Organisch-Chemisches Institut and Center for Multiscale Theory and Computation (CMTC), Universität Münster, Corrensstraße 40, 48149 Münster, Germany. E-mail: j.neugebauer@uni-muenster.de

16354 | *Phys. Chem. Chem. Phys.*, 2025, **27**, 16354–16370

This journal is © the Owner Societies 2025

solution of the **Z**-vector equations,[12–15] in addition to the standard TDDFT eigenvalue problem, to obtain relaxed density matrices (unless finite-field calculations are carried out), ΔSCF yields a set of occupied orbitals to characterize the electron density of a given state, from which the dipole moment can be calculated in precisely the same simple way as in the ground-state case. TDDFT excited-state dipole moments have been benchmarked and compared to various wavefunction-based methods by Loos, Jacquemin and co-workers.[16] Among the DFAs tested in that study, CAM-B3LYP produced the lowest average relative error of about 28%, while PBE0 and B3LYP showed errors of about 60% and, on average, significantly overestimated the magnitude of the excited-state dipole moments. Second-order methods like ADC(2) or CC(2) did not perform significantly better in general, while CCSD (either equation-of-motion or orbital-relaxed linear-response based) showed much lower relative errors around 10% on average. Ref. 16 also provides a valuable overview over previous studies on theoretical excited-state dipole moments.

While transition dipole moments from ΔSCF have been thouroughly investigated,[17] there is, to the best of our knowledge, no systematic benchmark of excited-state dipole moments from ΔSCF available to date. This is somewhat surprising, since ΔSCF methods have recently gained renewed attention as methods to calculate excited-state energies and properties.[1,18–20] As already indicated above, they exhibit technical advantages over TDDFT for property calculations,[15] as essentially ground-state methodology can be applied.[21] In addition, it is often argued that they are better suited in situations involving charge transfer, especially when employing DFAs which are not of range-separated hybrid type.[21–24] Another obvious advantage of ΔSCF methods is the possibility to describe double (and, in principle, even higher) excitations,[25] which are not accessible with standard TDDFT methods.

A conceptual issue arises in ΔSCF for open-shell low-spin states, including the important class of HOMO–LUMO (singly-excited) singlet excited states of molecules with closed-shell singlet ground-state: Typical ΔSCF methods describe the resulting excited state with a single Slater determinant (SD), leading to a so-called broken-symmetry solution, while several substituted SDs are needed to describe a true eigenstate of the squared total spin operator $\hat{S}^2$ in such a case. As argued in ref. 26 in the context of ferromagnetically vs. antiferromagnetically coupled spin centers, it can be expected that the charge distribution of such a broken-symmetry wavefunction is still a good representation of the true situation. By contrast, the spin density will be qualitatively wrong. Similar arguments can be made concerning applications of ΔSCF for excited electronic states, and it has in fact been shown that post-SCF spin purification usually improves the energetics of open-shell singlet states.[21] We would like to note, however, that not all excited states are necessarily (dominantly) open-shell states, in contrast to the statement made in ref. 22, which probably simply did not consider the following class of states: double excitations involving the simultaneous excitation of two electrons from one spatial orbital into another could very well be dominantly of closed-shell non-Aufbau type. In particular, HOMO → LUMO

double excitations starting from closed-shell singlet ground states, as will be studied in this work, will lead to a dominantly closed-shell singlet state.

Various types of ΔSCF-DFT methods have been proposed, e.g., the maximum-overlap method (MOM),[27] the initial maximum overlap method[28] (IMOM), the σ-SCF method,[29] the squared-gradient minimization technique (SGM),[25] or the state-targeted energy projection (STEP).[30] A difficulty that most of these variants have to avoid is variational collapse, where the desired excited determinant is not converged in favor of another one.[23] Related methods are the constricted variational density functional theory by Ziegler and co-workers[31] and the restricted open-shell Kohn–Sham (ROKS) method for low-spin excited states[32–34] that is based on Ziegler's sum method.[35] ROKS offers a way to describe spin-pure singlet excited states, since both a broken-symmetry and a triplet determinant are created from a common set of spatial orbitals. The quantity $2E_{BS} - E_T$ (containing the energy of the broken-symmetry and the triplet determinant) is minimized, which avoids the use of the energy-only spin-purification procedure that is sometimes performed in broken-symmetry ΔSCF approaches to achieve an energy correction.[34] Detailed reviews on ΔSCF-type approaches are provided in ref. 22 and 23.

In this work we aim at benchmarking the excited-state dipole moment of small to medium-sized organic molecules using ΔSCF to determine whether it can improve upon the shortcomings of TDDFT for this quantity, both in terms of magnitude and of orientation (if not dictated by symmetry). The work is structured as follows: after a short review of the methodological background, the employed benchmark sets for the open-shell singlet excitations are discussed. Then, the results for these excitations are shown and compared against TDDFT, (SCS-)CC2 and reference results from the literature.[16] Afterwards, we discuss several examples of long-range charge-transfer excitations. Note that in particular for this type of excited states, CC2 typically shows some shortcomings, which are mitigated by SCS-CC2.[36,37] Subsequently, IMOM results for double excitations are compared against linear-response(LR-)CCSDT results for a set of small molecules, before we conclude from our results.

2 Methodology

The dipole moment of a molecule described by a single-determinant wavefunction comprising a set of n orbitals $\{\phi_i\}$ is given by

$$\mu = \mu_{nuc} + \mu_{el} \tag{1}$$

$$= \sum_I^N Z_I \cdot \mathbf{R}_I - \int \rho(\mathbf{r})\mathbf{r}d\mathbf{r} \tag{2}$$

$$= \sum_I^N Z_I \cdot \mathbf{R}_I - \sum_i^n \langle \phi_i | \mathbf{r} | \phi_i \rangle, \tag{3}$$

where atomic units are used throughout (unless specified otherwise). The nuclear (μ_{nuc}) contribution to the electric dipole

This journal is © the Owner Societies 2025

Phys. Chem. Chem. Phys., 2025, **27**, 16354–16370 | **16355**

moment can trivially be evaluated in terms of the nuclear charge numbers Z_I and coordinates $\mathbf{R}_I$ of the N nuclei. The electronic (μ_{el}) component can be obtained either as the negative integral over the electron density $\rho(\mathbf{r})$ multiplied with the position operator $\mathbf{r}$, or equivalently by summing over the dipole molecular orbital (MO) integrals $\mathbf{r}_i := \langle \phi_i | \mathbf{r} | \phi_i \rangle$ for all occupied MOs.

While it is immediately clear that for closed-shell ground-state systems treated with SCF methods, simply the set of optimized ground-state orbitals $\{\phi_i^{(g)}\}$ should be employed for computing a consistent dipole moment, several more or less approximate routes can be followed for excited states described by a single Slater determinant. The most simple approximation corresponds to what is sometimes called ΔDFT, in which a non-Aufbau occupation is employed without further orbital relaxation. For a singly-excited state in which an occupied orbital ϕ_j is replaced by a virtual orbital ϕ_a, this amounts to computing,

$$\mu_{el}^{\Delta DFT} = \sum_{i,i \neq j}^{n} \left\langle \phi_i^{(g)} \middle| \mathbf{r} \middle| \phi_i^{(g)} \right\rangle + \left\langle \phi_a^{(g)} \middle| \mathbf{r} \middle| \phi_a^{(g)} \right\rangle. \quad (4)$$

This also corresponds to the dipole moment from a typical initial guess of a ΔSCF calculation. After orbital relaxation, the set of all (occupied and virtual) orbitals has changed from $\{\phi_r^{(g)}\} \rightarrow \{\phi_r^{(e)}\}$, so that we obtain

$$\mu_{el}^{\Delta SCF} = \sum_{i,i \neq j}^{n} \left\langle \phi_i^{(e)} \middle| \mathbf{r} \middle| \phi_i^{(e)} \right\rangle + \left\langle \phi_a^{(e)} \middle| \mathbf{r} \middle| \phi_a^{(e)} \right\rangle. \quad (5)$$

In arguably the most relevant case for ΔSCF, the superscript (e) would indicate a BS-type excited Slater determinant, which does not correspond to a pure spin state (as discussed above). Common spin purification schemes imply, however, that the density (though of course not the spin density) of this BS determinant should be similar to the one of the triplet determinant with the same/corresponding spatial orbitals occupied, so that

$$\mu_{el}^{\Delta SCF} \approx \mu_{el}^{triplet} = \sum_{i,i \neq j}^{n} \left\langle \phi_i^{(T)} \middle| \mathbf{r} \middle| \phi_i^{(T)} \right\rangle + \left\langle \phi_a^{(T)} \middle| \mathbf{r} \middle| \phi_a^{(T)} \right\rangle. \quad (6)$$

where superscript (T) now indicates that the orbitals are optimized for the triplet occupation. Another implication would be that a post-SCF spin-purification (SP; following the strategy for the corresponding energy correction) should not have a large effect,

$$\mu_{el}^{SP} = 2\mu_{el}^{\Delta SCF} - \mu_{el}^{triplet} \approx \mu_{el}^{\Delta SCF}. \quad (7)$$

Moreover, the differences between $\{\phi_r^{(e)}\}$, $\{\phi_r^{(T)}\}$, and the set of orbitals $\{\phi_r^{(ROKS)}\}$ obtained in a ROKS optimization of the open-shell singlet energy should be small. Hence, one might argue that the ROKS-based dipole moment,

$$\mu_{el}^{ROKS} = \sum_{i,i \neq j}^{n} \left\langle \phi_i^{(ROKS)} \middle| \mathbf{r} \middle| \phi_i^{(ROKS)} \right\rangle + \left\langle \phi_a^{(ROKS)} \middle| \mathbf{r} \middle| \phi_a^{(ROKS)} \right\rangle. \quad (8)$$

should be similar to $\mu_{el}^{triplet}$ and $\mu_{el}^{\Delta SCF}$ as well. In fact, large differences between these dipole moments might be a first indication for convergence to a wrong electronic state or a variational collapse.

One special comment applies to (long-range) charge-transfer excited states, in which the "donating" orbital ϕ_i is spatially separated from the "accepting" orbital ϕ_a. TDDFT using (semi-)local exchange–correlation approximations produces severe errors for the corresponding excitation energies. In particular, (i) the asymptotic value of the excitation energy is incorrect, since it is governed by the difference of the orbital energies involved, which suffer from an incorrect treatment of the integer discontinuity in (semi-)local XC potentials,[38] related to the fractional charge error.[39] And (ii), the long-distance behavior of the excitation energy as a function of the intermolecular distance does not follow the expected $-1/R$ behavior for a charge-separation process, since (semi-)local XC kernels cannot recover this behavior, which arises from the exact-exchange contribution in the TDDFT coupling matrix when using hybrid XC approximations (scaled by the percentage of exact exchange included).[40–43] In ΔSCF, long-range CT (LR-CT) excitation energies are obtained as differences of total energies, which may considerably improve the results for these classes of functionals. The situation may be more complicated for the dipole moment of an LR-CT state, though: for a pure single orbital-transition, "unrelaxed" TDDFT (neglecting the "relaxed density" contribution from the Z-vector equation) would yield an excited-state dipole moment similar to $\mu^{\Delta DFT}$, i.e., based on orbitals optimized for a neutral system. ΔSCF, by contrast, would yield an excited-state dipole moment for orbitals optimized in a charge-separated configuration, which will be subject to the fractional-charge problem.[39] In particular, this may lead to overdelocalization for (semi-)local exchange–correlation approximation (or global hybrids with a low percentage of exact exchange), unless other constraints prevent this effect.[44] Examples like donor–acceptor substituted polyene chains show, however, that the TDDFT results may be affected by additional issues, such as problems in the underlying ground-state calculation due to an incorrect behavior of the XC potential as well as incorrect relaxation contributions due to failures of the response function,[45–47] leading to an overall catastrophic behaviour of TDDFT excited-state dipoles from (semi-)local and global hybrid functionals.[48] Here, we will explore how ΔSCF deals with such cases (see Section 4.4).

3 Computational details

In the following, we consider open-shell singlet excitations for three different sets of molecules that have previously served as benchmarks of excited-state electronic-structure methods. The small-molecule set from ref. 16, the charge-transfer benchmark set from ref. 49, and the medium-sized molecule set from ref. 48 are considered here. For the first set, theoretical best estimates (TBEs: LR-CCSDT aug-cc-pVTZ with corrections from CCSTQ 6-31+G(d)) have been taken from ref. 16. In addition, TDDFT dipole moments for this set were available in ref. 16 for

16356 | *Phys. Chem. Chem. Phys.*, 2025, **27**, 16354–16370

This journal is © the Owner Societies 2025

PBE0 and CAM-B3LYP and were also confirmed and used for this work. In TDDFT and ΔSCF calculations, we applied the exchange–correlation approximations PBE0,[50] PBE,[51] CAM-B3LYP,[52] ωB97M-V,[53] and LC-ωPBE.[54] Regarding the latter two functionals, ω was kept at the default for ωB97M-V and set to 0.2 a.u. for LC-ωPBE. Since not all combinations of functionals and methods [IMOM, ROKS, (SCS-)CC2, TDDFT dipole moments] were available in our default choices for quantum chemistry software, we employed different programs for different combinations as outlined in the following. ΔSCF IMOM calculations were carried out for the first three functionals using SERENITY,[55,56] version 1.6.0,[57] making use of XCFun[58] and libint.[59] Restricted open-shell Kohn–Sham calculations (ROKS) were performed with QCHEM[60] (version 6.1) using the SGM algorithm. All IMOM and TDDFT calculations involving the latter two functionals were also performed with QCHEM. TDDFT calculations were carried out with ORCA, version 5.0.3,[61,62] in the case of the CAM-B3LYP functional, and with TURBOMOLE, version 7.4.1[63,64] otherwise. "Unrelaxed" excited-state dipole moments from TDDFT (i.e., neglecting the relaxation effect obtained from solving the Z-vector equations) were obtained with SERENITY,[55,56] version 1.6.1.[65] For reference purposes, we also computed (relaxed) spin-component-scaled- (SCS) CC2 excited-state dipole moments with TURBO-MOLE. The aug-cc-pVTZ basis set has been employed for these three test sets. For the charge-transfer excitations studied, also the cc-pVTZ basis set has been used.

In addition, we considered HOMO–LUMO double excitations of nitroxyl (HNO), formaldehyde, and nitrosomethane as previously studied in ref. 66 as well as of nitrous acid, borole, and cyclopentadienone considered before in ref. 67. Since no excited-state dipole moments had been included in ref. 66 and 67, we performed reference LR-CCSDT/6-31+G* calculations for these double excitations with the program MRCC.[68–70] The corresponding ΔSCF IMOM calculations were performed with the same basis sets, respectively, and the PBE0 functional. The geometries were taken from ref. 66 and 67.

4 Results

4.1 Benchmark sets and selection of excited states

Assessing excited-state dipole moments from approximate methods such as ΔSCF or TDDFT comes with several challenges. A practical challenge is to define a suitable measure for the error, since the dipole moments may be rather large in some cases, but close to zero in others. As has been discussed by Hait and Head–Gordon for the case of ground-state dipole moments from DFT,[11] a regularized relative error criterion may be well suited in such a case, in which a relative error is calculated for dipole moment magnitudes above a certain threshold value (1 D in that work), whereas absolute errors are considered below that threshold. Here, we follow the strategy by Jacquemin and co-workers[16] and report both absolute and relative errors, but leave out cases in which the reference excited-state dipole moment $|\mu_{exc}^{ref}| < 0.15$ D in the latter case. Such cases only occur in the first

benchmark set introduced below, and we provide the corresponding non-regularized relative errors for that set in the ESI† for completeness. Another important aspect discussed by Jacquemin and co-workers[16] is the consequence of state-mixing in approximate excited-state methods: if one includes cases in the statistics in which state-mixing clearly obscures the results, the errors will be dramatically higher (and potentially useless) than when concentrating on the well-behaved cases. In the context of ΔSCF, state-mixing can be extreme especially for higher-lying states, up to the point that one variationally collapses to a lower-lying state of entirely different character. Hence, it seems more adviseable to concentrate on well-behaved cases, in which at least the state assignment is rather unproblematic. The dipole-moment errors for these cases can then be discussed separately from the difficulties of optimizing more challenging excited electronic states. ΔSCF benchmark studies are often restricted to HOMO–LUMO transitions, which seem to be rather well-behaved in this context. For instance, a benchmark study on transition dipole moments using ΔSCF investigated only the HOMO–LUMO excitations of 107 molecules.[17] The same argument was also made in ref. 71, where HOMO–LUMO excitations were favored for investigating the accuracy of ΔSCF calculations. These examples could indicate that ΔSCF methods are more difficult to converge for higher-lying excitations, so that such excitations are frequently avoided in ΔSCF studies. Hence, we follow the same strategy and mostly concentrate on HOMO–LUMO-type excited states here. But in addition, we also consider a small set of doubly excited states to analyze the accuracy of ΔSCF for this class of excited states unattainable for standard TDDFT approximations.

The benchmark set from ref. 16, which contains 46 open-shell singlet excited states of 18 molecules, was selected as a first benchmark set. Among the 18 HOMO–LUMO excited states, two have a dipole moment of net zero, so that 16 excitations are remaining from this set. The corresponding molecules are shown in Fig. 1.

The second set comprises the HOMO–LUMO excitations of the charge-transfer (CT) benchmark set from ref. 49. It is shown in Fig. 2; for this set, CC2/aug-cc-pVTZ data are available from that reference, which we confirmed with our calculations. Also this set contains molecules of rather high symmetry, so that the orientations of the excited-state dipole moments are fixed.

A third set was chosen as a subset of the molecules studied in ref. 72, which include slightly larger molecules (see Fig. 3); excited-state dipole moments from CC2 and TDDFT (including PBE0 and CAM-B3LYP) with an aug-cc-pVTZ basis for the molecules of our set 3 have been investigated and compared already in ref. 48, and we have convinced ourselves that our data agree with those from that reference. For these molecules, the direction of the dipole moment is not dictated by symmetry, which offers another criterion to assess the ΔSCF dipole moment.

SCF convergence in ΔSCF calculations is often more difficult than in the corresponding ground-state calculations, one obvious reason being the problem of variational collapse, and

This journal is © the Owner Societies 2025

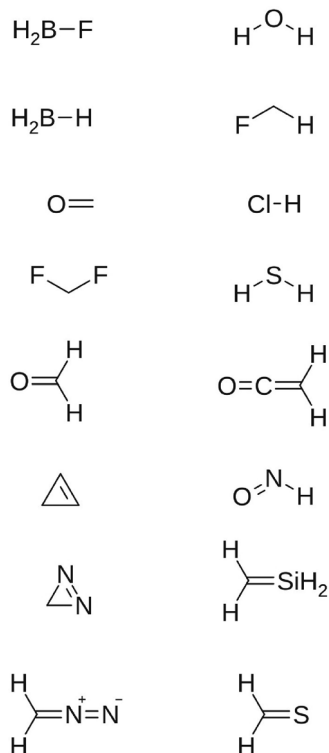Phys. Chem. Chem. Phys., 2025, 27, 16354–16370 | 16357

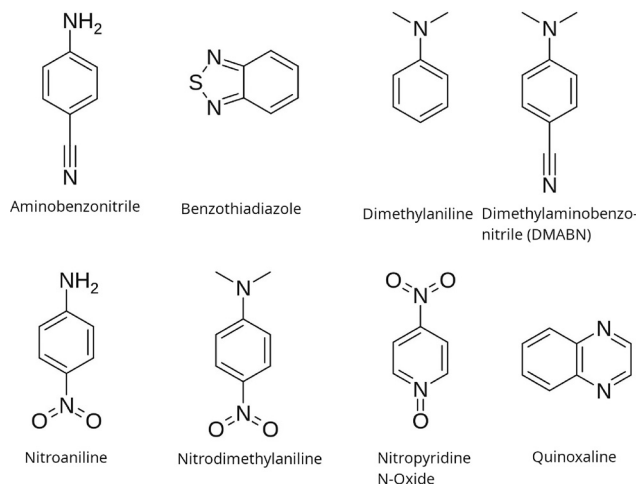Fig. 1   Molecules of benchmark set 1 (from ref. 16).

Fig. 2   Molecules of benchmark set 2 (from ref. 49).

another one the possible convergence to another undesired state. As a consequence, some of the combinations of ΔSCF strategy and functional could not successfully be converged, which in turn affects the statistical comparison. In our calculations, this was mainly a problem observed for the long-range corrected functionals: for set 1, the IMOM LC-ωPBE calculations involving the molecules cyclopropane, H_2S, HCl and HNO did not converge to the desired excited state, in spite of different attempts involving different initial guesses and optimization strategies. Similarly, the calculations for cyclopropane using the ωB97M-V functional failed for both IMOM and ROKS,

and also the combination ωB97M-V ROKS did not yield the proper state for diazomethane and H_2S. For set 2, IMOM did not converge to the desired excited states with both these functionals for aminobenzonitrile, dimethylaniline, and DMABN, and also the ωB97M-V ROKS calculation for nitrodimethylaniline could not be converged to the desired state. But also TDDFT calculations can be problematic regarding an unambiguous assignment of the target states. Here, we observed a highly mixed transition for molecule 4 of set 3 with PBE as well as for dimethylaniline of set 2 with ωB97M-V. It is also to be noted that due to the diffuse basis functions present in the aug-cc-pVTZ basis set, a number of excitations had to be identified manually, since additional orbitals appear between the orbitals that correspond to the HOMO and LUMO for the cc-pVTZ basis set (without diffuse functions) in a few cases, in particular for set 2. Since the problematic SCF convergence considerably affected the statistical basis for LC-ωPBE and ωB97M-V, we mainly discuss the functionals PBE, PBE0, and CAM-B3LYP in the main text, but will mention the general trends observed with the additional functionals where appropriate. All available data for these functionals are provided in the ESI† in addition.

Since TBEs are available for the excited state dipole moments of set 1, we were able to assess the quality of CC2 and SCS-CC2 for that set (see Fig. S1 and S2 in the ESI†). This is important regarding the use of these methods as a reference for sets 2 and 3. SCS-CC2 is more accurate with an average deviation of 5.4% from the TBE compared to 7.4% for CC2, which is consistent with the findings in ref. 37. The convergence of the excited state dipole moment with respect to basis set size is briefly investigated for six example molecules using the basis sets cc-pVDZ, cc-pVTZ, and aug-cc-pVTZ. The results are depicted in Fig. S5 in the ESI† and demonstrate that the differences between the different basis sets are rather modest, with the notable exception of H_2O, where augmentation of the basis leads to a rather drastic increase in the dipole moment. While excitation energies are not the focus of this work, these data were also obtained by calculating the excited states of interest. The average deviation of the excitation energies from the respective references for the three investigated sets of molecules can be found in the ESI.† It becomes apparent that TDDFT yields more accurate excitation energies than IMOM and ROKS in most cases. For the CAM-B3LYP functional, however, ROKS is similarly accurate for set 2 and 3.

4.2   HOMO–LUMO singlet excitations

We start with a comparison of the excited-state dipole moments for set 1. The corresponding values are given in Table 1. The sign of the dipole moment is provided in order to highlight possible sign changes between different methods; it refers to the orientation of the molecule in the reference structures (see Computational details). We would like to point out that the single-determinant treatment within ΔSCF approaches leads to an additional complication in case of the first four entries in Table 1: for those molecules, the lowest excited states are degenerate Π states, as they involve excitations from/to doubly degenerate π-type orbitals. ΔSCF approaches will typically break
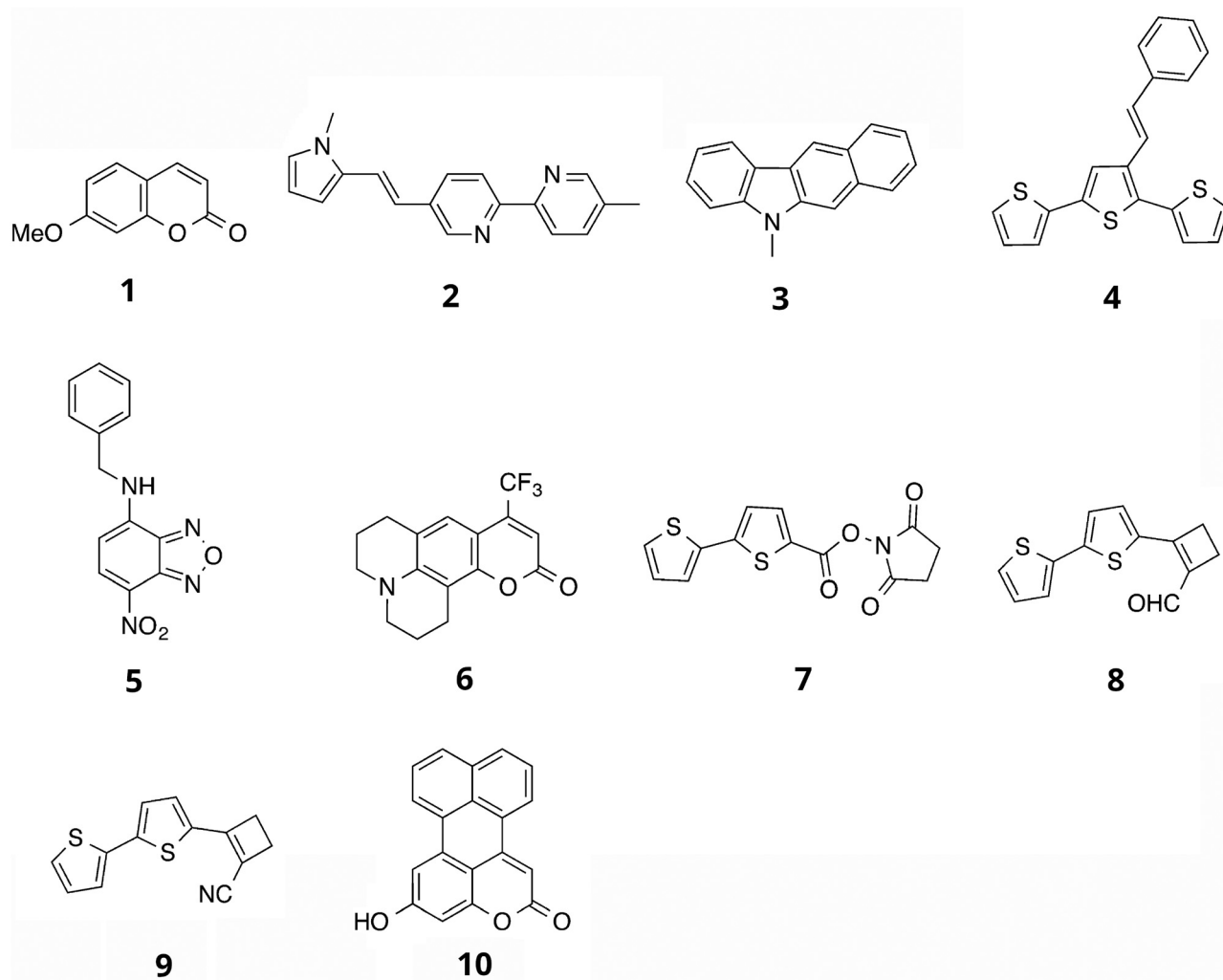
16358 | Phys. Chem. Chem. Phys., 2025, 27, 16354–16370

This journal is © the Owner Societies 2025

Fig. 3 Molecules of benchmark set 3 (from ref. 72).

Table 1 Excited state dipole moments (in Debye) of the IMOM, ROKS and TDDFT results and reference data from ref. 16 for set 1

Molecule	PBE			PBE0			CAM-B3LYP			TBE
	IMOM	ROKS	TDDFT	IMOM	ROKS	TDDFT	IMOM	ROKS	TDDFT	
BF	0.10	0.28	0.49	−0.04	0.15	0.33	−0.13	0.04	0.27	0.30
BH	0.43	0.53	0.49	0.43	0.51	0.51	0.42	0.48	0.49	0.56
CO	−0.58	−0.32	0.12	−0.84	−0.57	−0.26	−0.95	−0.70	−0.34	−0.13
HCl	−1.86	−2.11	−3.45	−2.13	−2.42	−2.87	−2.18	−2.42	−2.66	−2.50
CF$_2$	−0.16	0.06	0.31	−0.36	−0.15	0.04	−0.42	−0.23	−0.03	0.04
CH$_2$S	0.71	0.79	0.84	0.76	0.85	0.75	0.72	0.81	0.69	0.84
Cyclopropene	−0.71	−0.98	−1.49	−0.64	−0.96	−1.61	−0.58	−0.88	−1.09	−0.81
Diazirine	−2.42	−2.45	−2.42	−2.53	−2.56	−2.58	−2.59	−2.62	−2.67	−2.51
Diazomethane	−3.06	−3.05	−2.83	−3.20	−3.16	−3.01	−3.28	−3.23	−3.14	−3.28
Formaldehyde	1.30	1.31	1.31	1.30	1.29	1.36	1.36	1.35	1.43	1.32
H$_2$CSi	−2.16	−2.13	−1.81	−2.14	−2.12	−1.94	−2.08	−2.06	−1.90	−1.92
H$_2$O	−1.37	−1.48	−1.68	−1.55	−1.63	−1.65	−1.39	−1.43	−1.49	−1.56
H$_2$S	−1.65	−1.83	−2.41	−1.97	−2.12	−2.17	−1.82	−1.87	−1.86	−1.86
HCF	0.84	0.90	0.91	0.89	0.94	0.91	0.92	0.96	0.93	0.96
HNO	1.62	1.63	1.61	1.71	1.72	1.69	1.76	1.76	1.74	1.68
Ketene	−2.14	−2.12	−2.02	−2.46	−2.50	−2.32	−2.62	−2.66	−2.45	−2.39

this orbital degeneracy. Since the main benchmark sets of this work include systems of sizes up to 38 atoms, we employ SCS-CC2

as a method to calculate reference excited-state dipole moments, where other reference values are not available. In ref. 37 it has been

This journal is © the Owner Societies 2025

Phys. Chem. Chem. Phys., 2025, **27**, 16354–16370 | **16359**

shown that spin-component scaling yields this quantity with higher accuracy than CC2, in agreement with our findings discussed above.

The mean absolute percentage deviations (MAPDs) of the excited-state dipole moments μ_{exc} for the first set of molecules are shown in Fig. 4 to quantify the average relative error; the corresponding average absolute deviations can be found in Fig. S7 in the ESI.† As mentioned above already, the relative errors are excluded for cases where the reference value is smaller than 0.15 Debye, which concerns CF_2 and CO in the present case. The reference values are the theoretical best estimates (TBEs) from ref. 16. The relative errors without this regularization can be found in Fig. S9 in the ESI.† We also provide a comparison of excitation energies in Fig. S11–S14 in the ESI,† as this information was utilized, together with the dipole moments and (dominant) orbital transitions, to identify corresponding excited states in ΔSCF and TDDFT. It becomes apparent that TDDFT excited-state dipole moments show the largest variation with respect to the XC approximation chosen: especially with the GGA-type PBE functional, rather large average errors of 20.3% are obtained, while both standard and range-separated hybrids reduce this error considerably (13.5% for PBE0, 8.2% for CAM-B3LYP). For ΔSCF approaches, the results are much more uniform in this respect, with average relative errors between 15.6 and 19.4% for IMOM, and between

7.3 and 11.1% for ROKS. Especially for ROKS we note that CAM-B3LYP shows the largest error, while PBE yields a mean relative deviation that is considerably lower than in the TDDFT case. In the ESI† (Fig. S9), we also provide the corresponding data for LC-ωPBE and ωB97M-V. It can be seen that LC-ωPBE yields the lowest MAPD for ROKS at 7.8% while ωB97M-V has the lowest MAPD for TDDFT at 8.0%, keeping in mind, however, that these functionals have been evaluated with a limited statistics because of the above-mentioned convergence issues.

The excited-state dipole moments of the charge-transfer benchmark set 2 are listed in Table 2 in comparison to SCS-CC2/aug-cc-pVTZ data. Since no corresponding TBEs are available for these dipole moments, these SCS-CC2 values serve as our reference data in this case, keeping in mind that this may not be the optimum choice. The corresponding MAPDs are shown in Fig. 5; average absolute values can be found in Fig. S16 in the ESI.† Interestingly, the functional dependence in this case is rather weak for ROKS (between 11.4 and 15.1%) and TDDFT (between 7.8 and 12.7%), whereas IMOM shows much larger variations in the relative errors between the different functionals (from 8.6% for CAM-B3LYP up to 17.0% for PBE). It can be seen that changing from a GGA to a (global or range-separated) hybrid functional leads to a considerable improvement of the excited-state dipole moments, which is most pronounced for IMOM. For the other range-separated hybrid
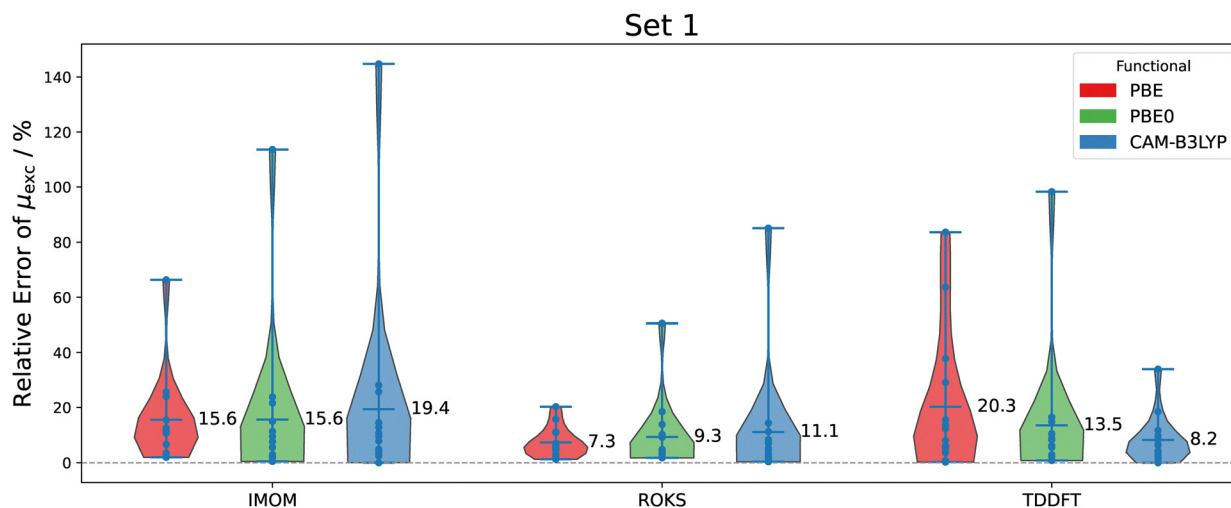

Fig. 4 Relative deviation (MAPD) of the excited-state dipole moments μ_{exc} of set 1 from the TBE[16] reference.

Table 2 Excited state dipole moments (in Debye) of the IMOM, ROKS, TDDFT, and SCS-CC2 results for set 2

Molecule	PBE			PBE0			CAM-B3LYP			SCS-CC2
	IMOM	ROKS	TDDFT	IMOM	ROKS	TDDFT	IMOM	ROKS	TDDFT	
Aminobenzonitrile	−9.11	−9.33	−9.31	−9.47	−9.34	−8.97	−9.42	−9.05	−8.66	−9.71
Benzothiadiazole	−3.55	−3.67	−5.06	−4.18	−4.58	−5.09	−4.64	−5.20	−4.92	−4.92
Dimethylaniline	−5.05	−5.10	−6.19	−5.22	−5.51	−5.46	−5.35	−5.82	−4.83	−4.53
DMABN	−11.00	−11.11	−11.80	−11.50	−11.06	−11.32	−11.52	−10.82	−10.90	−12.19
Nitroaniline	−12.29	−12.51	−12.15	−13.25	−12.35	−12.86	−13.72	−12.05	−12.88	−14.14
Nitrodimethylaniline	−14.29	−14.11	−13.76	−15.30	−13.71	−14.60	−15.78	−13.42	−14.61	−16.23
Nitropyridine-*N*-oxide	4.74	4.52	4.92	5.04	4.25	5.15	4.75	—	4.42	4.30
Quinoxaline	−2.83	−3.13	−4.66	−3.61	−4.18	−4.71	−4.16	−4.76	−4.58	−5.24

16360 | *Phys. Chem. Chem. Phys.*, 2025, **27**, 16354–16370

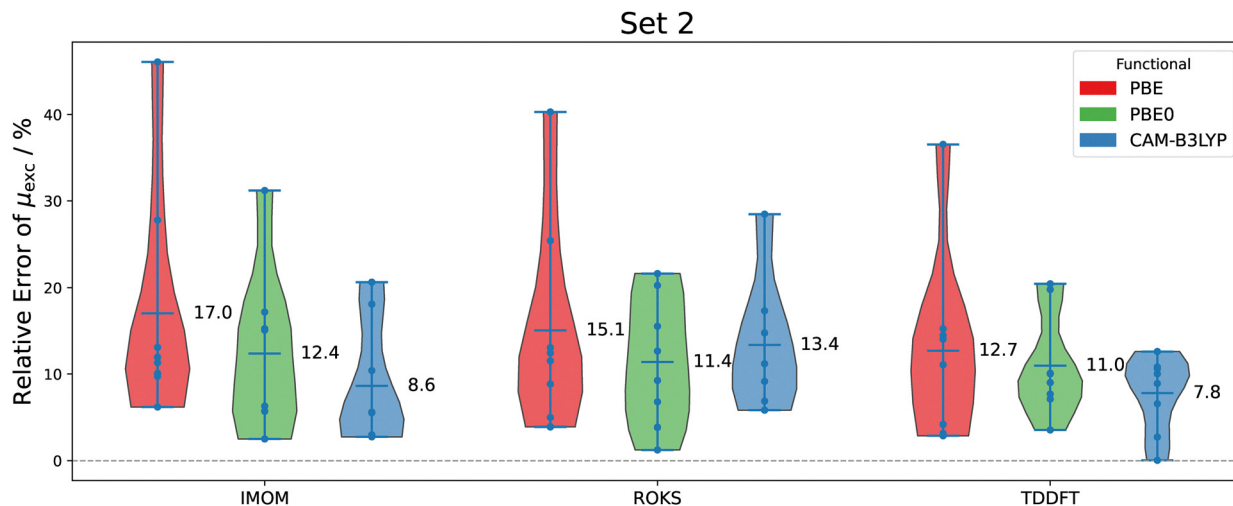This journal is © the Owner Societies 2025

Fig. 5 Relative deviation (MAPD) of the excited-state dipole moments of set 2 from the SCS-CC2 reference.

functionals investigated in this work (see Fig. S15 in the ESI†), the ROKS and TDDFT results do not show a significant impovement copmared to CAM-B3LYP; the IMOM data are not entirely conclusive for LC-ωPBE and ωB97M-V, as the proper excited state of interest could only be converged for 5 out of the 8 molecules of this set. When looking at the absolute values of the excited-state dipole moments of the individual molecules of set 2 in Table 2, it becomes apparent that the DFT methods tested here often underestimate the CC2 values (and also the SCS-CC2 reference). This is in line with earlier findings based on TDDFT.[48,73]

Absolute values of the excited-state dipole moments for set 3 are given in Table 3, and the corresponding MAPDs are shown in Fig. 6. We noted that the PBE/TDDFT calculation for molecule 4 led to strong state-mixing, making it essentially impossible to identify the desired electronic state. Since also the PBE0/TDDFT calculation is affected by this problem, even if to a lesser extent, and since the excited-state dipole moment of this molecule is rather small, the relative errors in Fig. 6 are computed omitting molecule 4 of this set. Also for the discussion of the angle deviations (see below), it turned out that molecule 4 introduces a heavy bias in this set, and so it has been omitted at that point as well. The full data including molecule 4 are provided as additional material in the ESI† (Fig. S25–S28).

For this set of molecules, none of the combinations of excited-state method and functional yields an error below 13%, the only exception being TDDFT with PBE0. For IMOM, we again observe that more sophisticated functionals lead to smaller errors, and also for ROKS, hybrid functionals lead to smaller errors than the non-hybrid PBE approximation. However, in case of ROKS there is no improvement by changing from a standard global hybrid to a range-separated hybrid; on the contrary, the error is slightly larger for ROKS with CAM-B3LYP than with PBE0. For the CAM-B3LYP functional, IMOM and TDDFT perform similarly well with an MAPD of about 14% MAE, while the corresponding ROKS error is somewhat higher with 17.3%. The other range-separated hybrids investigated provide no clear improvement over CAM-B3LYP in this case. As can be seen by comparison to the data in Fig. S25 in the ESI,† omitting molecule 4 leads to a decrease in the relative error in all cases, with TDDFT-PBE0 benefitting most (the TDDFT-PBE value is left unchanged since no data could be assigned in this case).

Since the molecules in this set possess lower symmetry, the direction of the excited-state dipole moment vector can serve as another quality measure. The angle deviations for the individual molecules are provided in Section S5.8 in the ESI.† Looking at this data, it becomes apparent that most of the calculations show quite low angle deviations near 5 degrees. Only a few

Table 3 Absolute values of excited state dipole moments (in Debye) of the IMOM, ROKS, TDDFT, and SCS-CC2 results for set 3

Molecule	PBE			PBE0			CAM-B3LYP			SCS-CC2
	IMOM	ROKS	TDDFT	IMOM	ROKS	TDDFT	IMOM	ROKS	TDDFT	
1	5.98	6.37	7.65	6.41	6.80	6.89	6.61	6.90	6.61	7.09
2	4.95	5.05	12.64	5.63	5.15	8.59	5.88	4.92	5.66	7.73
3	3.12	3.17	4.02	3.31	3.24	3.69	3.54	3.11	3.46	3.44
4	0.92	0.90	—	0.87	0.73	1.47	0.74	0.82	0.71	0.56
5	12.43	12.85	12.34	12.81	13.10	12.30	12.70	12.84	12.43	13.48
6	11.62	11.47	13.06	12.73	11.56	13.06	13.26	11.39	12.17	14.19
7	3.06	2.66	3.94	3.86	3.89	5.32	3.96	3.64	4.11	5.86
8	6.66	6.86	10.24	7.08	7.14	6.50	7.31	7.09	7.36	8.55
9	5.99	6.15	9.51	6.39	6.47	7.60	6.57	6.45	6.76	8.61
10	4.93	5.24	5.24	5.41	5.90	5.89	5.82	6.48	6.14	6.28

This journal is © the Owner Societies 2025

Phys. Chem. Chem. Phys., 2025, **27**, 16354–16370 | **16361**
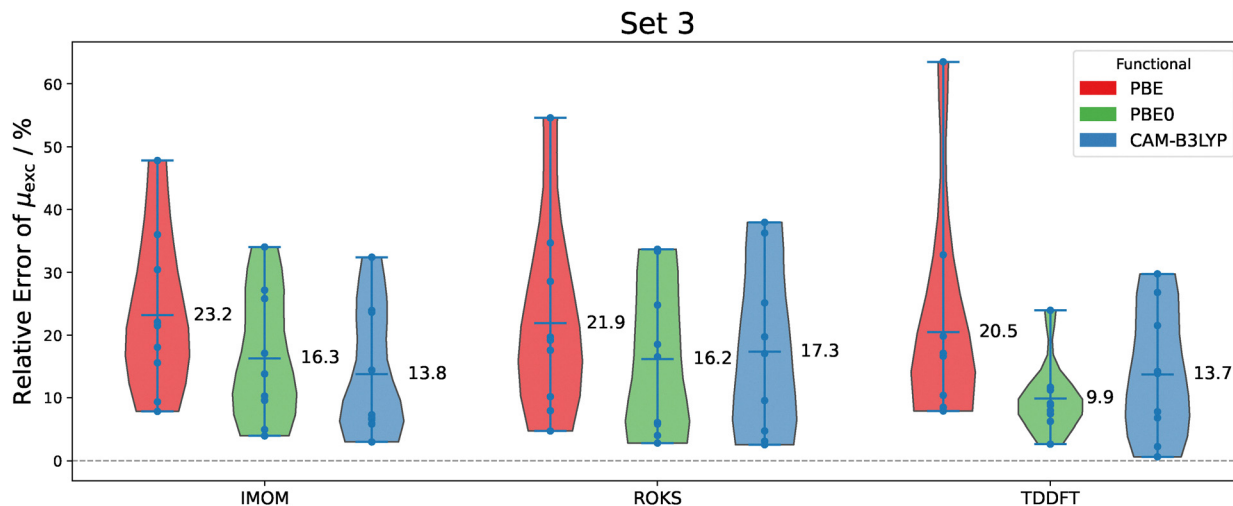
Set 3

Fig. 6 Relative deviation (MAPD) of the excited-state dipole moments μ_{exc} of set 3 from the SCS-CC2 reference. Note that molecule 4 was omitted here.

outliers with larger errors stand out, in particular molecule 4 with deviations above 30 degrees. The large angle error for molecule 4 may be related to its overall small magnitude of the excited-state dipole moment (see Table 3). Since this would heavily bias a comparison of the angle deviations, we provide and discuss here the average angles obtained when omitting molecule 4, see Table 4. The average angles computed when considering the full set of molecules can be found in Table S16 in the ESI.† As can be seen from Table 4, the average angle deviations for all methods/functionals are below 10 degrees, and for most of the cases considered here, they are even close to or below 5 degrees. PBE apparently yields the largest errors for this quantity, at least in case of TDDFT and IMOM calculations. Including molecule 4 into the statistics confirms the generally better performance of the hybrid functionals, but increases the average errors to close to 8 degrees or more in all cases.

In addition, we also investigated the difference dipole moment ($\Delta\vec{\mu} = \vec{\mu}_{\text{Exc}} - \vec{\mu}_{\text{GS}}$). The individual excited-state as well as ground-state dipole moment components are listed in the Tables S7–S9 in the ESI.† The average angle deviation from the SCS-CC2 difference dipole moments is shown in Table 5, again omitting molecule 4.

For this quantity, the functional dependence is more pronounced: the average deviation varies between about 10–18 degrees for PBE and 5–6 degrees for CAM-B3LYP. The other range-separated hybrid functionals yield comparable results

Table 4 Average angles (in degrees) between the excited-state dipole moments of the IMOM, ROKS and TDDFT calculations respectively, and the SCS-CC2 reference of set 3. Note that molecule 4 is omitted here

Functional	IMOM	ROKS	TDDFT
PBE	5.6	5.5	8.3
PBE0	4.6	4.9	3.2
CAM-B3LYP	4.5	5.7	4.3
LC-ωPBE	4.1	4.8	4.0
ωB97M-V	4.9	6.6	5.4

Table 5 Average angles (in degrees) between the difference dipole moments of the IMOM, ROKS and TDDFT calculations respectively, and the SCS-CC2 reference of set 3. Note that molecule 4 is omitted here

Functional	IMOM	ROKS	TDDFT
PBE	12.7	10.1	18.0
PBE0	8.2	5.4	11.5
CAM-B3LYP	5.2	6.0	5.2
LC-ωPBE	7.6	5.7	7.8
ωB97M-V	6.7	8.0	4.2

with difference dipole angles below 8 degrees. Also here, including molecule 4 leads to a significant increase in the average error, so that all PBE values are between 15 and 20 degrees, and also PBE0 as well as LC-ωPBE yield errors between 10 and 20 degrees for all three excited-state variants considered here.

The MAD and MAPD of CC2 compared to SCS-CC2 have also been calculated for set 2 and set 3. They can be found in Fig. S5 and S6 in the ESI.† Both in absolute and relative terms, the deviations are much lower compared to the deviation between the DFT methods in this work and SCS-CC2.

Generally, the performance of IMOM and ROKS for the excited-state dipole moment can be rated to be broadly similar based on the results of this work. ROKS performs slighty better for set 1, where high-quality reference data are available, while IMOM achieves lower deviations for set 2 and slightly lower deviations for set 3 (taking SCS-CC2 as a reference). The angle deviations for set 3 for IMOM and ROKS are similar, while ROKS performs slightly better for angles between difference dipole moments. It may seem surprising at first glance that IMOM does not show worse results than ROKS, at least for sets 2 and 3, despite the unresolved spin contamination. But this could be related to the lower quality of the SCS-CC2 reference data for these sets.

4.3 Spin-purification effects on excited-state dipole moments

In order to further analyze this issue, we investigated the effect of the spin-purification formula given in eqn (7) on the

16362 | *Phys. Chem. Chem. Phys.*, 2025, **27**, 16354–16370

This journal is © the Owner Societies 2025

Table 6 Excited state dipole moments (in Debye) of the IMOM, IMOM including spin purification (IMOM-SP), and ROKS results as well as reference TBE data from ref. 16 for a few examples of set 1

	IMOM	IMOM-SP	ROKS	TBE
BF	0.10	0.32	0.28	0.30
Cyclopropene	−0.71	−1.01	−0.98	−1.23
Diazomethane	−3.06	−3.09	−3.05	−3.28
Formaldehyde	1.30	1.34	1.31	1.32
H$_2$O	−1.37	−1.54	−1.48	−1.56

excited-state dipoles of some example molecules of test set 1 for the PBE functional. The results are shown in Table 6.

Hence, in all examples considered here, the spin-purification either leads to a considerable improvement (compared to the TBE) or has a small effect on the excited-state dipole moment anyway. In those cases where the effect is significant, also the agreement with ROKS is improved. Phenomenologically, this improvement stems from the fact that the triplet dipole moments are smaller in magnitude than the ones obtained from IMOM. Therefore, calculating the correction according to eqn (7) yields absolute values for the dipole moment that are higher than the IMOM solution. In case of large orbital relaxation effects in the triplet state, however, the situation may be different.

To further illustrate this correction, we show the difference density between the IMOM and the triplet densities in Fig. 7 for the water molecule contained in set 1.

4.4 A closer look at CT states

Especially the results for set 2 may seem somewhat surprising, since it is often argued that ΔSCF is better suited for CT excitations than TDDFT.[21–24,74] However, this argument primarily refers to excitation energies, whereas the effects of approximations in ΔSCF and TDDFT may have different consequences for the excited-state dipole moment. Jacquemin reported in ref. 48 that beneficial error cancellation effects may occur in TDDFT-based excited-state dipole-moment calculations using global hybrid functionals like PBE0. In fact, we observe for our set 2 here that excited-state dipole moments for CT excitations are more accurately captured by TDDFT in

Fig. 7 Difference density $\rho_{IMOM}(\mathbf{r}) - \rho_{T_1}(\mathbf{r})$ of the water molecule of set 1 using the PBE functional and aug-cc-pVTZ basis set. Positive areas are colored in yellow and negative areas in dark grey. The isovalue is $\pm 5 \times 10^{-4}$.

general (with the exception of CAM-B3LYP) than by IMOM or ROKS calculations employing the same XC approximation.

To further analyze this issue, we re-investigate the cases of α,ω-NH$_2$,NO$_2$-polyene chains from ref. 48, which have been studied there with TDDFT based on different XC functionals. The TDDFT results for BLYP (from ref. 48), CAM-B3LYP, and ωB97M-V are shown in Fig. 8 (left) along with our SCS-CC2 data and the CC2 data. The latter correspond to the reference data from ref. 48, whereas we consider SCS-CC2 a more reliable reference here for the reasons outlined above. In Fig. 8 (right), the corresponding IMOM results are shown. It becomes obvious that using IMOM for the GGA functional BLYP instead of TDDFT avoids the exaggerated excited-state dipoles, and the IMOM/BLYP value for $N = 15$ agrees with the CC2 reference data. However, the CC2 values have a maximum at $N = 13$, which is only observed with TDDFT when functionals of the RS-hybrid type, such as CAM-B3LYP are employed. Extrapolating the IMOM CAM-B3LYP data, one may speculate that a similar maximum will be found for slightly larger values of N. The ωB97M-V functional, however, does show a maximum at $N = 13$ with IMOM, and a maximum at $N = 11$ with TDDFT. This is qualitatively in line also with the SCS-CC2 reference data, which show a maximum at $N = 11$, and are in reasonable agreement with the IMOM values from CAM-B3LYP and (in particular) ωB97M-V. The emergence of a maximum points to two opposing effects that vary with the chain length, which might be the increasing electron–hole distance in the CT state due to the increasing length of the molecular chain, and the increasing delocalization of the involved molecular orbitals, which counteracts the former effect.

In Fig. 9, we compare the frontier molecular orbitals for the longest polymer $N = 15$ studied here. In the BLYP-TDDFT calculation, the corresponding excitation is clearly dominated by the HOMO–LUMO transition (weight: 83%). The corresponding singly occupied MOs in the BLYP-IMOM calculation on the HOMO–LUMO excited state are considerably more delocalized, indicating that (i) the IMOM calculation on this zwitterionic state suffers considerably more from the overdelocalization error than the ground-state SCF forming the basis for the TDDFT calculation and, (ii) this, in combination with the overestimation of the ground-state dipole moment observed in ref. 48 may lead to an error cancellation, bringing the IMOM excited-state dipole moments into closer agreement with the CC2 reference values here. Since also the IMOM B3LYP calculations are in better qualitative agreement with the reference than the corresponding TDDFT results, similar error cancellation effects may also be at work for this functional. The overestimation of ground-state dipole moments (and other field-response properties) has already been investigated in detail before for these types of systems.[47] In particular for the ground-state dipole moments, non-hybrid exchange approximations were found to severely overestimate the charge transfer between the donor and acceptor groups. This was qualitatively traced back to the failure observed for the polarizability of unsubstituted polyenes,[46] assuming that the donor/acceptor pair acts as a source of an external electric field. The range-separated
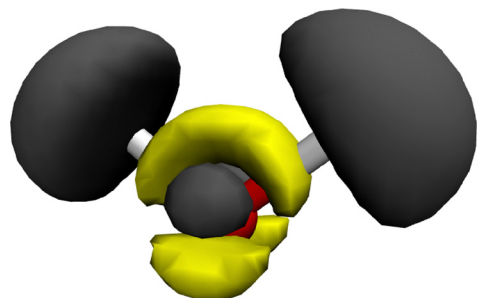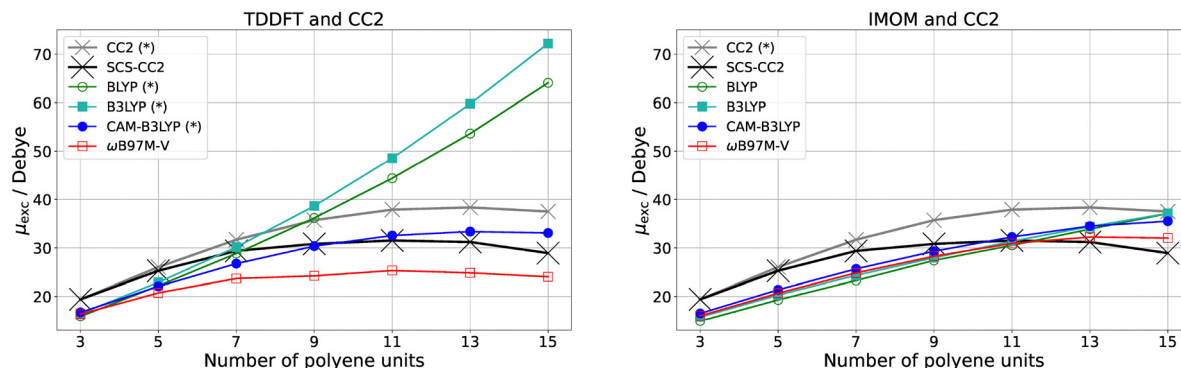
This journal is © the Owner Societies 2025

Phys. Chem. Chem. Phys., 2025, **27**, 16354–16370 | **16363**

Fig. 8 Excited state dipole moments of donor–acceptor-substituted polyenes $H_2N-[HC=CH-]_N NO_2$ with N = 3–15 units using various different exchange–correlation approximations. Left: TDDFT; right: IMOM; CC2 and SCS-CC2 data are given for comparison. Data sets indicated with a star (*) have been taken from ref. 48.
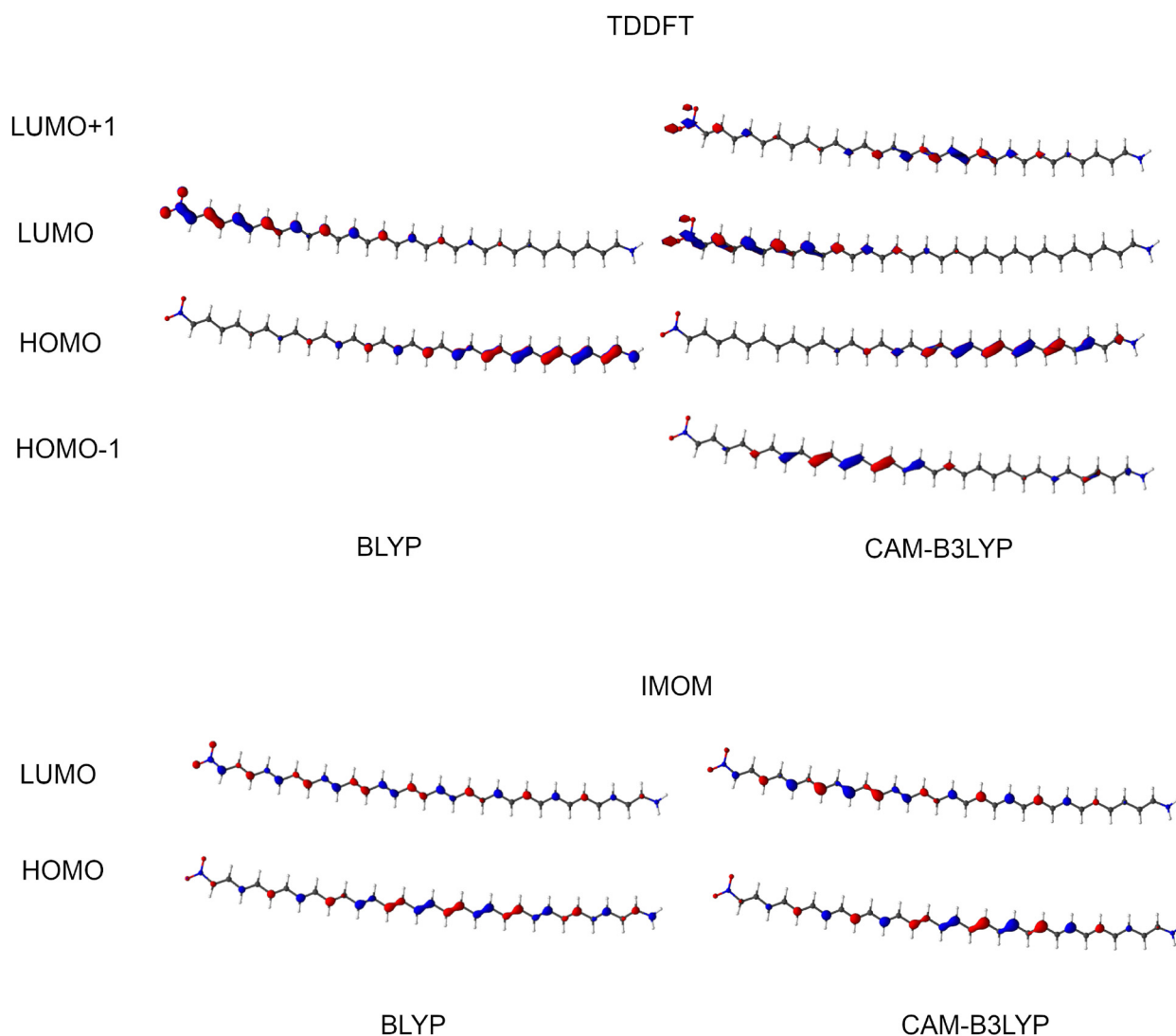

Fig. 9 Frontier molecular orbitals involved in the lowest singlet $\pi \rightarrow \pi^*$ excitation of the N14-polyene obtained with BLYP and CAM-B3LYP (basis: aug-cc-pVDZ). Top: Orbitals from a ground-state SCF calculation as employed in the TDDFT case; bottom: orbitals from a ΔSCF (IMOM) calculation.

hybrids considered here do not show a dramatic TDDFT error in case of longer chain lengths, and in turn no dramatic improvement based on error cancellation can be expected in the IMOM case.

16364 | *Phys. Chem. Chem. Phys.*, 2025, **27**, 16354–16370

This journal is © the Owner Societies 2025

We also note that the CAM-B3LYP HOMO and LUMO as employed in the TDDFT calculation (*i.e.*, the orbitals optimized for the ground state) are only slightly less delocalized than in the BLYP case, and hence cannot alone explain the qualitatively different behavior of the TDDFT-based excited-state dipole moments. But in the CAM-B3LYP TDDFT case, the HOMO–LUMO orbital transition has a weight of only 46% in the excitation. In addition, also the HOMO–(LUMO+1) and (HOMO−1)–LUMO transitions contribute with 22% and 21%, respectively, which can partially explain the smaller excited-state dipole moment.

As another extreme case, we consider the dipole moment of HOMO → LUMO excited singlet state of the ethylene–tetra-fluoroethylene dimer at a distance of 8 Å. The involved orbitals are visualized in Fig. 10.

On top of the previously discussed methods, the excited-state dipole moments were also calculated with additional methods, namely TDDFT within the Tamm–Dancoff approximation, unrelaxed TDDFT excited-state dipole moments, and a procedure where the orbital occupation is changed just like in ΔSCF, but where the orbitals are not relaxed. We denote the
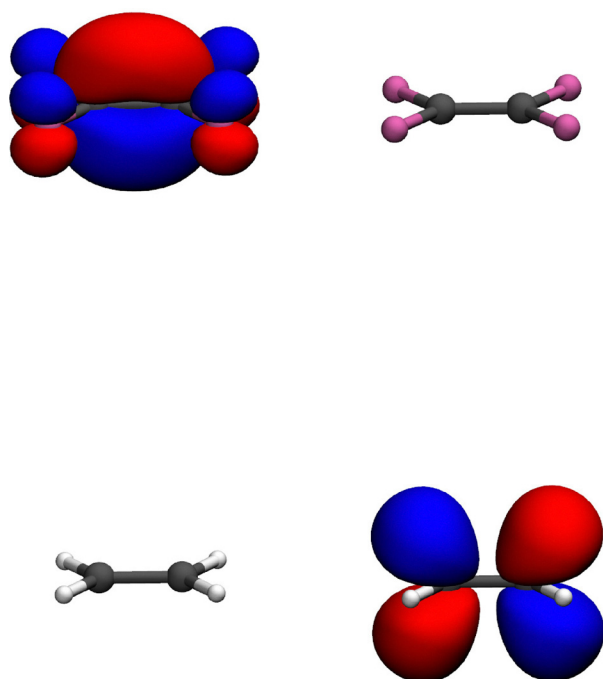

Fig. 10 Visualization of the HOMO (left) and LUMO (right) of the ethylene–tetrafluoroethylene dimer at a distance of 8 Å using PBE/cc-pVTZ (isovalue: 0.05).

latter procedure as ΔDFT in the following. Results for PBE, PBE0, and CAM-B3LYP with a cc-pVTZ basis are shown in Table 7, including reference SCS-CC2 values. In addition, we provide PBE and PBE0 excited-state dipole moments obtained with the aug-cc-pVTZ basis in Table 8.

While all methods employed here agree on a dipole moment of 38.0 ± 0.5 Debye if the smaller cc-pVTZ basis is used, some differences can be observed for the aug-cc-pVTZ basis: while all the TDDFT and also the ΔDFT excited-state dipole moments are still between 36.2 and 38.4 Debye, the ROKS and IMOM dipole moments decrease to values between 35.9 and 28.7 Debye. This can be traced back again to an overdelocalization problem in this zwitterionic state, which apparently is suppressed in the smaller cc-pVTZ basis. In Fig. S33 in the ESI,† we show the HOMO of the IMOM PBE case (corresponding to the ground-state LUMO) to illustrate this problem. Orbital contributions on the C_4F_4 moiety can clearly be recognized. To test for possible variational-collapse effects to the ground state, we also computed the MO overlap matrices between the ground and the IMOM and ROKS excited states for the PBE/aug-cc-pVTZ basis, respectively, which are shown as heat maps in Fig. S34–S36 in the ESI.† It can clearly be recognized from those figures that a HOMO–LUMO substitution has taken place, while there are no other significant occupied-virtual overlaps. In addition, symmetry arguments speak against a simple variational collapse in this case, as the ground-state LUMO (IMOM HOMO) is anti-symmetric with respect to the mirror plane perpendicular to the carbon–carbon axes, whereas the ground-state HOMO is symmetric.

4.5 Double excitations

As a next step, we investigate double excitations using the IMOM ΔSCF method. We took the geometries of the molecules nitroxyl, formaldehyde, and nitrosomethane from ref. 66, and the geometries of nitrous acid, borole and cyclopentadienone from ref. 67, and calculated their closed-shell HOMO–LUMO double excitation by imposing a non-Aufbau closed-shell initial guess after having performed a ground-state calculation. To obtain reference values, we performed LR-CCSDT calculations, which reproduce the calculations in ref. 66 and 67. The obtained excitation energies and dipole moments can be found in Tables 9 and 10 respectively. The absolute MAEs of the ΔSCF excitation energies from the TBE and the MAEs and MAPDs of the excited state dipole moments are shown in Table 11.

From Table 11 it becomes apparent that the excitation energies calculated with ΔSCF are on average closer to the exFCI (selected configuration interaction calculations extrapolated

Table 7 Excited state dipole moment magnitudes of the HOMO−LUMO excitation of the ethylene−tetrafluoroethylene dimer (in Debye) calculated with several methods (basis: cc-pVTZ)

| Distance | SCS-CC2 | XC functional | TDDFT | | TDA | ROKS | IMOM | ΔDFT |
			Relaxed	Unrelaxed				
8 Å	38.00	PBE	38.07	38.41	38.07	37.95	37.95	38.42
		PBE0	38.06	38.38	38.06	37.97	37.97	38.42
		CAM-B3LYP	38.02	38.32	38.02	37.99	37.98	38.41

This journal is © the Owner Societies 2025

Phys. Chem. Chem. Phys., 2025, **27**, 16354–16370 | **16365**

Table 8 Excited state dipole moment magnitudes of the HOMO–LUMO excitation of the ethylene–tetrafluoroethylene dimer (in Debye) calculated with several methods (basis: aug-cc-pVTZ)

Distance	XC functional	TDDFT		TDA	ROKS	IMOM	ΔDFT
		Relaxed	Unrelaxed				
8 Å	PBE	37.91	38.39	37.91	28.65	33.05	38.39
	PBE0	36.25	36.70	36.37	35.89	32.81	38.25

Table 9 Excitation energies of the HOMO–LUMO double excitations (in eV)

Method	HNO	HCHO	MeNO	HNO$_2$	Borole	Cyclopentadienone
LR-CCSDT	4.82	11.10	5.26	8.50	5.07	7.07
IMOM PBE0	4.37	10.38	4.77	7.92	4.86	6.20
IMOM CAM-B3LYP	4.31	10.42	4.71	7.80	5.03	6.37
IMOM ωB97M-V	4.34	10.37	4.72	7.83	5.06	6.44
IMOM LC-ωPBE	4.27	10.16	4.70	7.94	4.76	6.07
exFCI[a]/TBE[b]	4.51[a]	10.45[a]	4.86[a]	8.17[b]	4.71[b]	6.85[b]

[a] Ref. 66. [b] Ref. 67.

Table 10 Excited state dipole moments of the HOMO–LUMO double excitations (in Debye)

Method	HNO	HCHO	MeNO	HNO$_2$	Borole	Cyclopentadienone
LR-CCSDT	1.95	1.02	2.53	2.22	2.31	4.09
IMOM PBE0	1.95	0.63	2.52	2.74	2.69	5.55
IMOM CAM-B3LYP	1.98	0.67	2.59	2.77	2.72	5.76
IMOM ωB97M-V	1.97	0.65	2.57	2.74	2.76	5.74
IMOM LC-ωPBE	1.91	0.77	2.46	2.73	2.64	5.40

Table 11 Absolute deviations of the excitation energies from the TBE and absolute and relative deviations of the excited state dipole moments from the LR-CCSDT calculations of the HOMO–LUMO double excitations

Method	ΔE_{exc}/eV	$\Delta\mu$/Debye	$\Delta\mu$/%
LR-CCSDT	0.38	—	—
IMOM PBE0	0.23	0.46	19
IMOM CAM-B3LYP	0.26	0.51	20
IMOM ωB97M-V	0.25	0.51	20
IMOM LC-ωPBE	0.29	0.42	16

to full CI, see ref. 66), and TBE values[67] than the LR-CCSDT calculations, with errors between 0.23 and 0.29 eV for the different functionals, compared to 0.38 eV for LR-CCSDT. ΔSCF double excitation calculations for HNO, HCHO and MeNO have previously been reported in the literature,[25] however, without considering the corresponding dipole moment. It can be seen that the excited-state dipole moments of doubly excited states can approximately be predicted using the ΔSCF IMOM method. On average, the ΔSCF dipole moment deviates from the LR-CCSDT dipole moment by 0.42–0.51 Debye, which corresponds to a relative average deviation of 16–20%. Compared to the results for singly excited states, this error is larger than the relative PBE0 IMOM error for set 1 and 3, but similar to the relative error for set 2. In order to have more certainty about the accuracy of the excited-state dipole moments, it would be necessary to calculate their values with an even more accurate method than LR-CCSDT, especially since the excitation energies of the ΔSCF calculation were closer to excFCI/TBE values from the literature.[66,67] In addition, the LR-CCSDT

excitation energies still contain deviations of a few tenths of an eV compared to the theoretical best estimates reported in ref. 66.

Another point to discuss is the use of the comparatively small 6-31+G* basis set, since it is likely that the excited-state dipole moment has not converged in this respect.[75] In Tables S20 and S21 in the ESI,† we present additional data for two of the molecules (HNO and MeNO) using the larger aug-cc-pVDZ basis and the PBE0 and CAM-B3LYP functionals. The effect on excitation energies and excited-state dipole moments is qualitatively similar for all methods. For instance, the LR-CCSDT excited-state dipole moment decreases by about 0.37 and 0.34 Debye for HNO and MeNO, respectively, while the corresponding changes for ΔSCF PBE0 are 0.32 and 0.26 Debye.

We also determined the angles between the IMOM excited-state dipole moments and the LR-CCSDT reference in those cases where the dipole orientation is not determined by symmetry. The angle between the PBE0 IMOM and LR-CCSDT excited-state dipole moments is very small for HNO and MeNO with 3.1 and 1.2 degrees, respectively. For CAM-B3LYP, these values are even lower at 1.0 and 0.3 degrees. For HNO$_2$, the deviation in orientation is slightly larger with an angle of 8.7 (7.9) degrees.

5 Conclusions and outlook

In this work, we have assessed the performance of ΔSCF methods to predict the excited-state dipole moments of

16366 | *Phys. Chem. Chem. Phys.*, 2025, **27**, 16354–16370

This journal is © the Owner Societies 2025

HOMO–LUMO excited singlet states of three sets of molecules, ranging from small to medium-sized molecules, as well as of additional CT and doubly excited states.

It was found that for the investigated PBE, PBE0 and CAM-B3LYP functionals, the ΔSCF methods IMOM and ROKS are, depending on the set, competitive with TDDFT, although they often do not offer a clear advantage over TDDFT for singly excited states. As demonstrated for examples from the first test set, applying a spin purification to the excited-state dipole moments may have a beneficial effect for IMOM dipole moments. The long-range corrected functionals ωB97M-V and LC-ωPBE usually are comparable in accuracy with CAM-B3LYP, and may offer improvement in individual cases.

The deviations in excited-state dipole moment directions were also investigated, as well as the directions of difference dipole moments, which have implications for the application of oriented external electric fields (OEEFs). Since OEEFs may be used to selectively stabilize one electronic state relative to another one and hence to tune excited-state reactivity/selectivity, and since a predicted stabilization depends on the magnitude and orientation of the (difference) dipole moments, predictive calculations should be able to yield both accurate magnitudes and orientations of excited-state and difference dipole moments. Since angle deviations have been found to be low on average with all DFT-based methods here, with only a few outliers, this aspect seems to be less relevant in practice than the errors in the magnitude of the dipole moments.

The excited-state dipole moments calculated with SCS-CC2 qualitatively agree, but may differ by a few tenths of a Debye from the CC2 data. TDDFT and IMOM with range-separated hybrids in turn agree with the SCS-CC2 values qualitatively. For the case of push–pull-substituted polyenes, we could demonstrate that IMOM avoids the catastrophic chain-length dependence of the excited-state dipole moments observed in TDDFT calculations employing (semi-)local exchange–correlation approximations or global hybrids with low percentage of exact exchange. In fact, the results for up to 15 double-bond units are in reasonable agreement with the SCS-CC2 reference values. However, this is most likely due to a beneficial error cancellation effect, as the significant overdelocalization error for the zwitterionic excited state seems to reduce the excited-state dipole moment and hence to counteract the overestimation of charge-transfer in the ground state observed in earlier studies.[46,47]

Regarding practial guidance for ΔSCF calculations aiming at reliable excited-state dipole moments, we observe that hybrid functionals (global or range-separated) provided better results on average for our sets 2 and 3, while PBE resulted in the lowest MAPD for set 1, both for ROKS and for IMOM. Concerning the direction of the excited-state dipoles and difference dipoles, we found that ωB97M-V and CAM-B3LYP provide the best agreement with the SCS-CC2 reference data, which is important regarding the applications of OEEFs as mentioned above. These functionals also lead to the closest agreement, especially regarding the chain-length-dependence, for the push–pull-substituted polyenes. In general, the analysis is complicated by the fact that individual, exceptionally large relative errors may occur in cases of small absolute values, and the regularization applied for the MAPDs may thus introduce a rather strong bias. Of practical relevance is also that the range-separated hybrids, in particular those with 100% exact exchange asymptotically, showed more severe convergence problems for the cases investigated here. In some cases, this can be overcome by starting from initial guesses obtained as ΔSCF solutions with, *e.g.*, other functionals, but several problematic cases could not be resolved in this way.

For the six investigated double excitations, the IMOM results show a mean error of about 16–20% for the excited-state dipole moments compared to LR-CCSDT reference calculations, which is not significantly higher than the deviations observed for the singly-excited states. In particular, it demonstrates that qualitative and at lease semi-quantitative information about excited-state dipole moments can be obtained for double excitations with ΔSCF.

Although this work was supposed to focus on simply benchmarking the excited-state dipole moment, it has become apparent that the question of convergence to the correct state needs to be answered as well. A criterion is needed to characterize whether a ΔSCF calculation converged on the desired excited state in order to decide if a given deviation from a proposed reference value is due to the inaccuracy of the description in that specific case or if it is due to converging on a different excited state or solution altogether. Future work will have to address this aspect.

Conflicts of interest

There are no conflicts of interest to declare.

Data availability

The data supporting this article have been included as part of the ESI.†

Acknowledgements

References

1 L. Kunze, A. Hansen, S. Grimme and J.-M. Mewes, PCM-ROKS for the Description of Charge-Transfer States in Solution: Singlet-Triplet Gaps with Chemical Accuracy from Open-Shell Kohn-Sham Reaction-Field Calculations, *J. Phys. Chem. Lett.*, 2021, **12**, 8470–8480.

2 A. Sirohiwal and D. A. Pantazis, Electrostatic profiling of photosynthetic pigments: implications for directed spectral tuning, *Phys. Chem. Chem. Phys.*, 2021, **23**, 24677–24684.

3 D. Hait, Y. H. Liang and M. Head-Gordon, Too big, too small, or just right? A benchmark assessment of density functional theory for predicting the spatial extent of the

This journal is © the Owner Societies 2025

Phys. Chem. Chem. Phys., 2025, **27**, 16354–16370 | **16367**

electron density of small chemical systems, *J. Chem. Phys.*, 2021, **154**, 074109.

4 S. Shaik, D. Mandal and R. Ramanan, Oriented electric fields as future smart reagents in chemistry, *Nat. Chem.*, 2016, **8**, 1091–1098.

5 M. Garavelli, Computational organic photochemistry: strategy, achievements and perspectives, *Theor. Chem. Acc.*, 2006, **116**, 87–105.

6 P. Liu and E. W. Miller, Electrophysiology, Unplugged: Imaging Membrane Potential with Fluorescent Indicators, *J. Am. Chem. Soc.*, 2020, **53**, 11–19.

7 G. Tian, F. Qiu, C. Song, S. Duan and Y. Luo, Electric Field Controlled Single-Molecule Optical Switch by Through-Space Charge Transfer State, *J. Phys. Chem. Lett.*, 2021, **12**, 9094–9099.

8 F. Müh, M. E.-A. Madjet, J. Adolphs, A. Abdurahman, B. Rabenstein, H. Ishikita, E.-W. Knapp and T. Renger, α-Helices direct excitation energy flow in the Fenna-Matthews-Olson protein, *Proc. Natl. Acad. Sci. U. S. A.*, 2007, **104**, 16862–16867.

9 M. Romei, C.-Y. Lin, I. Mathews and S. Boxer, Electrostatic control of photoisomerization pathways in proteins, *Science*, 2020, **367**, 76–79.

10 M. M. T. El-Tahawy, I. Conti, M. Bonfanti, A. Nenov and M. Garavelli, Tailoring Spectral and Photochemical Properties of Bioinspired Retinal Mimics by in Silico Engineering, *Angew. Chem., Int. Ed.*, 2020, **59**, 20619–20627.

11 D. Hait and M. Head-Gordon, How Accurate Is Density Functional Theory at Predicting Dipole Moments? An Assessment Using a New Database of 200 Benchmark Values, *J. Chem. Theory Comput.*, 2018, **14**, 1969–1981.

12 F. Furche and R. Ahlrichs, Adiabatic time-dependent density functional methods for excited state properties, *J. Chem. Phys.*, 2002, **117**, 7433–7447.

13 D. Marx and J. Hutter, *Ab Initio Molecular Dynamics – Basic Theory and Advanced Methods*, Cambridge University Press, Cambridge, 2009.

14 A. Kovyrshin and J. Neugebauer, Analytical gradients for excitation energies from frozen-density embedding, *Phys. Chem. Chem. Phys.*, 2016, **18**, 20955–20975.

15 J. M. Herbert, Visualizing and characterizing excited states from time-dependent density functional theory, *Phys. Chem. Chem. Phys.*, 2024, **26**, 3755–3794.

16 R. Sarkar, M. Boggio-Pasqua, P.-F. Loos and D. Jacquemin, Benchmarking TD-DFT and wave function methods for oscillator strengths and excited-state dipole moments, *J. Chem. Theory Comput.*, 2021, **17**, 1117–1132.

17 S. Bourne Worster, O. Feighan and F. R. Manby, Reliable transition properties from excited-state mean-field calculations, *J. Chem. Phys.*, 2021, **154**, 124106.

18 L. Kunze, T. Froitzheim, A. Hansen, S. Grimme and J.-M. Mewes, ΔDFT Predicts Inverted Singlet-Triplet Gaps with Chemical Accuracy at a Fraction of the Cost of Wave Function-Based Approaches, *J. Phys. Chem. Lett.*, 2024, **15**, 8065–8077.

19 T. Froitzheim, L. Kunze, S. Grimme, J. M. Herbert and J.-M. Mewes, Benchmarking Charge-Transfer Excited States in TADF Emitters: ΔDFT Outperforms TD-DFT for Emission Energies, *J. Phys. Chem. A*, 2024, **128**, 6324–6335.

20 L. Kunze, A. Hansen, S. Grimme and J.-M. Mewes, The Best of Both Worlds: ΔDFT Describes Multiresonance TADF Emitters with Wave-Function Accuracy at Density-Functional Cost, *J. Phys. Chem. Lett.*, 2025, **16**, 1114–1125.

21 M. W. D. Hanson-Heine, M. W. George and N. A. Besley, Calculating excited state properties using Kohn-Sham density functional theory, *J. Chem. Phys.*, 2013, **138**, 064101.

22 J. M. Herbert in *Theoretical and Computational Photochemistry*, ed. C. García-Iriepa and M. Marazzi, Elsevier, 2023, pp. 69–118.

23 D. Hait and M. Head-Gordon, Orbital Optimized Density Functional Theory for Electronic Excited States, *J. Phys. Chem. Lett.*, 2021, **12**, 4517–4529.

24 E. Selenius, A. E. Sigurdarson, Y. L. A. Schmerwitz and G. Levi, Orbital-Optimized Versus Time-Dependent Density Functional Calculations of Intramolecular Charge Transfer Excited States, *J. Chem. Theory Comput.*, 2024, **20**, 3809–3822.

25 D. Hait and M. Head-Gordon, Excited State Orbital Optimization via Minimizing the Square of the Gradient: General Approach and Application to Singly and Doubly Excited States *via* Density Functional Theory, *J. Chem. Theory Comput.*, 2020, **16**, 1699–1710.

26 F. Neese, Prediction of molecular properties and molecular spectroscopy with density functional theory: From fundamental theory to exchange-coupling, *Coord. Chem. Rev.*, 2009, **253**, 526–563, Theory and Computing in Contemporary Coordination Chemistry.

27 A. T. Gilbert, N. A. Besley and P. M. Gill, Self-consistent field calculations of excited states using the maximum overlap method (MOM), *J. Phys. Chem. A*, 2008, **112**, 13164–13171.

28 G. M. J. Barca, A. T. B. Gilbert and P. M. W. Gill, Simple Models for Difficult Electronic Excitations, *J. Chem. Theory Comput.*, 2018, **14**, 1501–1509.

29 H.-Z. Ye, M. Welborn, N. D. Ricke and T. Van Voorhis, σ-SCF: A direct energy-targeting method to mean-field excited states, *J. Chem. Phys.*, 2017, **147**, 214104.

30 K. Carter-Fenk and J. M. Herbert, State-targeted energy projection: A simple and robust approach to orbital relaxation of non-Aufbau self-consistent field solutions, *J. Chem. Theory Comput.*, 2020, **16**, 5067–5082.

31 J. Cullen, M. Krykunov and T. Ziegler, The formulation of a self-consistent constricted variational density functional theory for the description of excited states, *Chem. Phys.*, 2011, **391**, 11–18.

32 I. Frank, J. Hutter, D. Marx and M. Parrinello, Molecular dynamics in low-spin excited states, *J. Chem. Phys.*, 1998, **108**, 4060–4069.

33 M. Filatov and S. Shaik, Spin-restricted density functional approach to the open-shell problem, *Chem. Phys. Lett.*, 1998, **288**, 689–697.

34 T. Kowalczyk, T. Tsuchimochi, P.-T. Chen, L. Top and T. Van Voorhis, Excitation energies and Stokes shifts from a restricted open-shell Kohn-Sham approach, *J. Chem. Phys.*, 2013, **138**, 164101.

16368 | *Phys. Chem. Chem. Phys.*, 2025, **27**, 16354–16370

This journal is © the Owner Societies 2025

35 T. Ziegler, A. Rauk and E. J. Baerends, On the Calculation of Multiplet Energies by the Hartree-Fock-Slater Method, *Theor. Chim. Acta*, 1977, **43**, 261–271.

36 A. Tajti, B. Kozma and P. G. Szalay, Improved Description of Charge-Transfer Potential Energy Surfaces via Spin-Component-Scaled CC2 and ADC(2) Methods, *J. Chem. Theory Comput.*, 2021, **17**, 439–449.

37 A. Hellweg, The accuracy of dipole moments from spin-component scaled CC2 in ground and electronically excited states, *J. Chem. Phys.*, 2011, **134**, 064103.

38 D. Tozer, Relationship between long-range charge-transfer excitation energy error and integer discontinuity in Kohn-Sham theory, *J. Chem. Phys.*, 2003, **119**, 12697–12699.

39 A. J. Cohen, P. Mori-Sánchez and W. Yang, Insights into current limitations of density functional theory, *Science*, 2008, **321**, 792–794.

40 A. Dreuw, J. L. Weisman and M. Head-Gordon, Long-range charge-transfer excited states in time-dependent density functional theory require non-local exchange, *J. Chem. Phys.*, 2003, **119**, 2943–2946.

41 A. Dreuw and M. Head-Gordon, Failure of Time-Dependent Density Functional Theory for Long-Range Charge-Transfer Excited States: The Zincbacteriochlorin-Bacteriochlorin and Bacteriochlorophyll-Spheroidene Complexes, *J. Am. Chem. Soc.*, 2004, **126**, 4007–4016.

42 O. Gritsenko and E. J. Baerends, Asymptotic correction of the exchange correlation kernel of time-dependent density functional theory for long-range charge-transfer excitations, *J. Chem. Phys.*, 2004, **121**, 655–660.

43 J. Neugebauer, O. Gritsenko and E. J. Baerends, Assessment of a Simple Correction for the Long-Range Charge-Transfer Problem in Time-Dependent Density-Functional Theory, *J. Chem. Phys.*, 2006, **124**, 214102.

44 A. Solovyeva, M. Pavanello and J. Neugebauer, Describing long-range charge-separation processes with subsystem density-functional theory, *J. Chem. Phys.*, 2014, **140**, 164103.

45 B. Champagne, E. A. Perpète, S. J. A. van Gisbergen, E.-J. Baerends, J. Snijders, C. Soubra-Ghaoui, K. A. Robins and B. Kirtman, Assessment of conventional density functional schemes for computing the polarizabilities and hyperpolarizabilities of conjugated oligomers: An ab initio investigation of polyacetylene chains, *J. Chem. Phys.*, 1998, **109**, 10489–10498.

46 S. J. A. van Gisbergen, P. R. T. Schipper, O. V. Gritsenko, E. J. Baerends, J. G. Snijders, B. Champagne and B. Kirtman, Electric Field Dependence of the Exchange-Correlation Potential in Molecular Chains, *Phys. Rev. Lett.*, 1999, **83**, 694–697.

47 B. Champagne, E. A. Perpète, D. Jacquemin, S. J. A. van Gisbergen, E.-J. Baerends, C. Soubra-Ghaoui, K. A. Robins and B. Kirtman, Assessment of Conventional Density Functional Schemes for Computing the Dipole Moment and (Hyper)polarizabilities of Push-Pull π-Conjugated Systems, *J. Phys. Chem. A*, 2000, **104**, 4755–4763.

48 D. Jacquemin, Excited-State Dipole and Quadrupole Moments: TD-DFT *versus* CC2, *J. Chem. Theory Comput.*, 2016, **12**, 3993–4003.

49 P.-F. Loos, M. Comin, X. Blase and D. Jacquemin, Reference Energies for Intramolecular Charge-Transfer Excitations, *J. Chem. Theory Comput.*, 2021, **17**, 3666–3686.

50 C. Adamo and V. Barone, *Chem. Phys. Lett.*, 1998, **298**, 113–119.

51 J. P. Perdew, K. Burke and M. Ernzerhof, *Phys. Rev. Lett.*, 1996, **77**, 3865–3868.

52 T. Yanai, D. P. Tew and N. C. Handy, A new hybrid exchange-correlation functional using the Coulomb-attenuating method (CAM-B3LYP), *Chem. Phys. Lett.*, 2004, **393**, 51–57.

53 N. Mardirossian and M. Head-Gordon, ωB97M-V: A combinatorially optimized, range-separated hybrid, meta-GGA density functional with VV10 nonlocal correlation, *J. Chem. Phys.*, 2016, **144**, 214110.

54 E. Weintraub, T. M. Henderson and G. E. Scuseria, Long-range-corrected hybrids based on a new model exchange hole, *J. Chem. Theory Comput.*, 2009, **5**, 754–762.

55 J. P. Unsleber, T. Dresselhaus, K. Klahr, D. Schnieders, M. Böckers, D. Barton and J. Neugebauer, *J. Comput. Chem.*, 2018, **39**, 788–798.

56 N. Niemeyer, P. Eschenbach, M. Bensberg, J. Tölle, L. Hellmann, L. Lampe, A. Massolle, A. Rikus, D. Schnieders, J. P. Unsleber and J. Neugebauer, The subsystem quantum chemistry program Serenity, *Wiley Interdiscip. Rev.:Comput. Mol. Sci.*, 2023, **13**, e1647.

57 D. Barton, *et al.* qcserenity/serenity: Release 1.6.0. 2023, DOI: **10.5281/zenodo.10143266**.

58 U. Ekström, *XCFun: A library of exchange-correlation functionals with arbitrary-order derivatives*, 2020, DOI: **10.5281/zenodo.3946698**.

59 E. F. Valeev, *Libint: A library for the evaluation of molecular integrals of many-body operators over Gaussian functions*, **https://libint.valeyev.net/**, 2021; version 2.7.0-beta6.

60 Y. Shao, Z. Gan, E. Epifanovsky, A. T. Gilbert, M. Wormit, J. Kussmann, A. W. Lange, A. Behn, J. Deng and X. Feng, *et al.*, Advances in molecular quantum chemistry contained in the Q-Chem 4 program package, *Mol. Phys.*, 2015, **113**, 184–215.

61 F. Neese, *Wiley Interdiscip. Rev.:Comput. Mol. Sci.*, 2012, **2**, 71–78.

62 F. Neese, Software update: The ORCA program system—Version 5.0, *Wiley Interdiscip. Rev.:Comput. Mol. Sci.*, 2022, **12**, e1606.

63 TURBOMOLE, a development of University of Karlsruhe and Forschungszentrum Karlsruhe GmbH, 1989–2007, TURBOMOLE GmbH, since 2007; available from **https://www.turbomole.org**.

64 S. G. Balasubramani, G. P. Chen, S. Coriani, M. Diedenhofen, M. S. Frank, Y. J. Franzke, F. Furche, R. Grotjahn, M. E. Harding and C. Hättig, *et al.*, TURBOMOLE: Modular program suite for ab initio quantum-chemical and condensed-matter simulations, *J. Chem. Phys.*, 2020, **152**, 184107.

65 D. Barton, *et al.* qcserenity/serenity: Release 1.6.1. 2024, DOI: **10.5281/zenodo.10838411**.

66 P.-F. Loos, M. Boggio-Pasqua, A. Scemama, M. Caffarel and D. Jacquemin, Reference energies for double excitations, *J. Chem. Theory Comput.*, 2019, **15**, 1939–1956.

This journal is © the Owner Societies 2025

Phys. Chem. Chem. Phys., 2025, **27**, 16354–16370 | **16369**

67 F. Kossoski, M. Boggio-Pasqua, P.-F. Loos and D. Jacquemin, Reference Energies for Double Excitations: Improvement and Extension, *J. Chem. Theory Comput.*, 2024, **20**, 5655–5678.

68 M. Kállay, P. R. Nagy, D. Mester, Z. Rolik, G. Samu, J. Csontos, J. Csóka, P. B. Szabó, L. Gyevi-Nagy and B. Hégely, *et al.*, The MRCC program system: Accurate quantum chemistry from water to proteins, *J. Chem. Phys.*, 2020, **152**, 074107.

69 M. Kállay, *et al.*, *Mrcc, a quantum chemical program suite written by*. **https://www.mrcc.hu**.

70 M. Kállay and J. Gauss, Calculation of excited-state properties using general coupled-cluster and configuration-interaction models, *J. Chem. Phys.*, 2004, **121**, 9257–9269.

71 T. Kowalczyk, S. R. Yost and T. V. Voorhis, Assessment of the ΔSCF density functional theory approach for electronic excitations in organic dyes, *J. Chem. Phys.*, 2011, **134**, 054128.

72 D. Jacquemin, I. Duchemin and X. Blase, 0-0 Energies Using Hybrid Schemes: Benchmarks of TD-DFT, CIS(D), ADC(2), CC2, and BSE/GW formalisms for 80 Real-Life Compounds, *J. Chem. Theory Comput.*, 2015, **11**, 5340–5359.

73 J. J. Eriksen, S. P. Sauer, K. V. Mikkelsen, O. Christiansen, H. J. A. Jensen and J. Kongsted, Failures of TDDFT in describing the lowest intramolecular charge-transfer excitation in para-nitroaniline, *Mol. Phys.*, 2013, **111**, 1235–1248.

74 E. Selenius, A. E. Sigurdarson, Y. L. A. Schmerwitz and G. Levi, Correction to "Orbital-Optimized Versus Time-Dependent Density Functional Calculations of Intramolecular Charge Transfer Excited States", *J. Chem. Theory Comput.*, 2025, **21**, 1014.

75 M. R. Silva-Junior, S. P. Sauer, M. Schreiber and W. Thiel, Basis set effects on coupled cluster benchmarks of electronically excited states: CC3, CCSDR (3) and CC2, *Mol. Phys.*, 2010, **108**, 453–465.

16370 | *Phys. Chem. Chem. Phys.*, 2025, **27**, 16354–16370

This journal is © the Owner Societies 2025